A. Uhl and P. Wild. Multi-stage Visible Wavelength and Near Infrared Iris Segmentation Framework. In A. Campilho and M. Kamel, editors, *Proceedings of the 9th International Conference on Image Analysis and Recognition (ICIAR'12)*, volume 7325 of *LNCS*, pages 1–10, Aveiro, Portugal, June 25–27, 2012. © Springer. doi: 10.1007/978-3-642-31298-4_1. The original publication is available at www.springerlink.com.

Multi-stage Visible Wavelength and Near Infrared Iris Segmentation Framework*

Andreas Uhl and Peter Wild

Multimedia Signal Processing and Security Lab
Department of Computer Sciences, University of Salzburg, Austria
{uhl,pwild}@cosy.sbg.ac.at

Abstract. This paper presents a multi-stage iris segmentation framework for the localization of pupillary and limbic boundaries of human eyes. Instead of applying time-consuming exhaustive search approaches, like traditional circular Hough Transform or Daugman's integrodifferential operator, an iterative approach is used. By decoupling coarse center detection and fine boundary localization, faster processing and modular design can be achieved. This alleviates more sophisticated quality control and feedback during the segmentation process. By avoiding database-specific optimizations, this work aims at supporting different sensors and light spectra, i.e. Visible Wavelength and Near Infrared, without parameter tuning. The system is evaluated by using multiple open iris databases and it is compared to existing classical approaches.

Keywords: Iris biometrics, segmentation, preprocessing

1 Introduction

Iris recognition uses patterns of the iris of an individual's eye for human identification and is considered to be one of the most accurate biometric modalities [2]. Traditional iris processing following Daugman's approach [5] extracts binary features after mapping the textural area between inner pupillary and outer limbic boundary into a doubly dimensionless representation. In this model, pixels are identified by their angular position and shift from pupillary to limbic boundary, see Fig. 1. This way, different pupil dilation caused by varying illumination conditions can largely be tolerated. Early segmentation techniques simply employed circular Hough Transform [17] to find a parameterization of the boundaries needed for the mapping process. However, iris images captured under more realistic, unsurveilled conditions cause problems. Noisy artefacts caused by blur, reflections, occlusions, and most notably oblique viewing angles may lead to severe segmentation errors. If such errors occur, subsequent recognition is almost impossible. Since iris segmentation is susceptible to poor image quality, efficient and fast segmentation of iris images is still an open research question [13].

While most proposed iris segmentation techniques (see [2] for a survey) follow holistic approaches optimizing the parameters for a more-or-less simple (circular,

* Supported by the Austrian FIT-IT Trust in IT-Systems, project no. 819382.

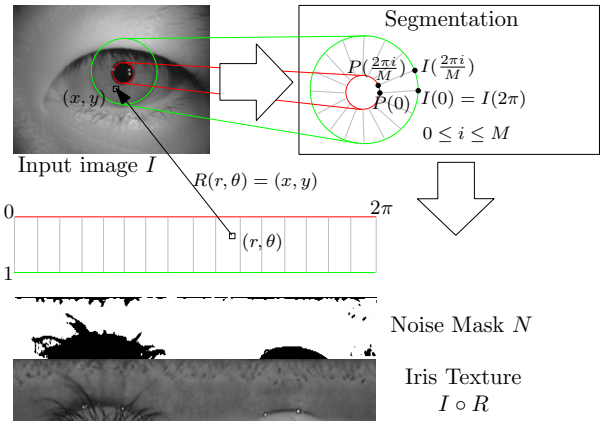

Fig. 1. Basic operation mode of iris segmentation.

elliptic) model of the iris, this paper presents a multi-stage iris segmentation framework decoupling the tasks of initial center detection and boundary fitting. More formally, we present a novel iris texture mapping function $R : [0, 1] \times [0, 2\pi] \rightarrow [0, m] \times [0, n]$ assigning each pair (r, θ) of pupil-to-limbic radial distance r and angle θ its originating location $R(r, \theta)$ within I. Note, that θ in this model refers to some parametrization of the iris boundary, not necessarily a circle, and that applications typically implement a discretized version. While we adopt Daugman's [5] solution $R(r, \theta) := (1 - r) \cdot P(\theta) + r \cdot L(\theta)$ establishing a linear combination of pupillary and limbic polar boundary curves $P, L : [0, 2\pi] \rightarrow [0, m] \times [0, n]$, the proposed segmentation framework concentrates on efficient and robust ways to obtain P and L. Instead of employing some sort of exhaustive searching or single error-prone strategies to derive P and L, this paper suggests to employ multi-stage iris segmentation for heterogeneous processing of visible wavelength (VW) and near infrared (NIR) imagery using the same processing technique. Especially for combinations of face and iris biometric modalities, there is a growing demand for iris segmentation techniques without strong assumptions on source image characteristics. Iris segmentation in VW frequently employs sclera search for approximate location [12], but this preprocessing raises problems in NIR because of lower contrast between sclera and skin. On contrary, NIR iris processing often relies on the pupil being easy localizable as a homogeneous dark region with high pupillary contrast, often violated in VW for dark irides. The proposed segmentation approach tries to build a very generic model without assumptions restricting the application to NIR or VW images.

This paper is organized as follows: Section 2 reviews related work regarding iris segmentation. Subsequently, the proposed framework is described in Section 3. Experiments are outlined in Section 4 using four different open iris-biometric databases and comparing results with two reference systems. Finally, Section 5 concludes this work.

2 Previous Work

According to the survey of Bowyer *et al.* [2], existing iris segmentation software in the field is largely based on two classical approaches with minor refinements only. Daugman's [5] approach applies exhaustive searching for center and radius using an integrodifferential operator to approximate P and L as circles. Wildes' [17] approach is similar, but uses binary edge maps and Hough Transform (HT), which is claimed to produce more stable results. The vast majority of known segmentation algorithms is based on these ideas and presents minor improvements [2]: for example, multi-resolution to speed up Hough transform, Canny edge detection to exclude unlikely boundary candidates, or histogram-based approaches for coarse pupil location and circle fit.

A significant modification to circular segmentation methods was introduced with active contours (AC) and active shape models (ASM). Abhyankar *et al.* [1] proposed ASM to account for inaccurate circular iris segmentation, especially for off-gaze iris images. ASMs use an idea similar to AC, looking for a contour minimizing an energy function composed of shape and image energy. While the image energy is defined in terms of the intensity difference on two sides of contour, shape energy tracks the difference between the current and average trained shape. Other approaches [6,15] have also identified the drawback of circular fitting, and use more complex shapes (like ellipses) or view-angle transformations to account for off-gaze.

The majority of iris recognition systems employ near infrared (NIR) imaging, capturing images at 700-900 nm wavelength, sacrificing pigment melanin information at the benefit of less reflections and even clearer texture information for heavily pigmented dark irides. However, recent challenges like the Noisy Iris Challenge Evaluation (NICE) now focus on the processing of visible-wavelength (VW) iris images. While images of the first type typically exhibit a very clear pupillary boundary, for the latter VW iris images, reflections, more heavily pigmented irides and typically smaller pupillary areas cause a much clearer limbic boundary. As a consequence, segmentation approaches are typically very different. Li *et al.* [9] and Chen *et al.* [4] implemented speed-ups of original HT reducing parameter space with a pre-location of the pupillary center. In available reference systems, this is a common practice to achieve acceptable segmentation time. However, there is high risk, that proposed heuristic preconditions do not hold in case of a change of sensors, especially from NIR to VW and vice versa. The approaches of Oroz *et al.* [10] and Labati *et al.* [8] explicitly try to avoid HT because of its huge processing time requirements and work with polar gradient-based approaches. This has the advantage, that oriented gradient masks may more effectively be applied. Iterative refinement of iris segmentation is alleviated and therefore polar image processing is also applied in our segmentation framework allowing also easy extension of modules to incorporate more sophisticated techniques for individual tasks. An example of a different implementation of single processing steps (relying on a weighted version of adaptive Hough transform), but following the proposed multi-stage approach has been published by the authors in [16].

3 Proposed Iris Segmentation Algorithm

The proposed iris segmentation algorithm divides the task of finding accurate pupillary and limbic boundary curves P, L into three subtasks: (1) image *enhancement*, (2) finding a *center point*, and (3) detecting *contours* given the approximate center as reference point. We consider this approach being a *framework*, since concrete implementations may refine either task of this processing chain building a concrete segmentation algorithm. The proposed reference implementation used in this work is illustrated in Fig. 2. Software uses the OpenCV[1] image library and is written in C++.

3.1 Image enhancement

The first task in the proposed processing chain enhances the input image by reducing the amount of noise able to degrade segmentation accuracy. While generally, determining a proper segmentation input resolution, reducing effects from defocus or motion blur may be implemented at this stage of processing, the current implementation concentrates on reflection removal. Hot spots caused by the use of flash, pupillary reflections of windows or other objects emitting light can be suppressed by looking for small objects with high luminance values. While the sclera in eye images typically represents the area with highest luminance in VW, in NIR the sclera is typically much darker. Still, reflections can be accurately identified by size filtering.

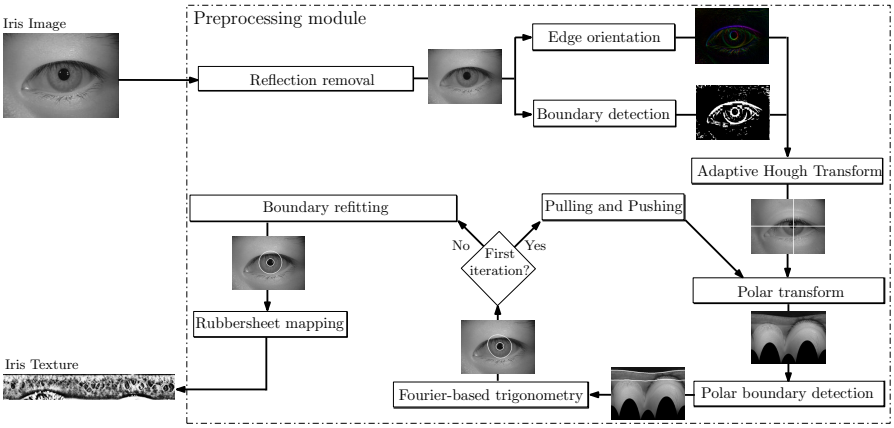

Fig. 2. Proposed segmentation framework: reflections are removed, an adaptive HT uses both gradient orientation and magnitude to estimate a center of multiple concentric rings, limbic and pupillary boundaries are detected in polar images and iteratively refined.

[1] Intel, Willow Garage: Open Source Computer Vision Library, `http://opencv.willowgarage.com`

For reflection removal, all pixels with intensities higher than the 0.85 quantile are selected, morphologically dilated using a circular 10×10 structuring element in 2 iterations and resulting regions are size-filtered rejecting all regions exceeding a total size of 2000 pixels. This is necessary to keep small reflection spots only and avoid inpainting of the sclera region. Inpainting is a very time consuming step. All selected regions are reconstructed from their boundary using *Navier-Stokes* inpainting.

3.2 Center point detection

The next task computes an approximate position of the iris center, which is basically any point completely inside the limbic L and pupillary P boundary, exploiting the fact that the required eye center is the unique center of multiple concentric rings. Using this definition, the center of an eye is not unique - ideally, a center point should be close to the centers of circles approximating L and P. An advantage of this method is, that it enables transparent processing for NIR and VW images since typically either pupil (NIR) or iris boundary (VW) may contribute to a larger extent to the center search. To alleviate center search, gradient magnitude and orientation is computed from the enhanced image. We employ Adaptive Hough Transform [3] for iterative center detection using a 10×10 accumulator grid with 0.5 pixel precision threshold:

1. The accumulator is initialized and candidate points obtained from the gradient image are evaluated. In addition to the reference implementation [3], to select initial candidate points, not only edge orientation is estimated (using horizontal and vertical 3×3 Sobel kernels), but a boundary edge mask is calculated from the top 20 percent of most intensive edge points (using magnitude) in Gaussian blurred gradient images rejecting all candidates within cells of a 30×30 grid with no dominant mean orientation (i.e. the magnitude of the mean orientation is less than 0.5). By this modification we avoid gradient information from eyelashes, which will exhibit an almost equal amount of high edges with opposite directions.
2. All candidate points whose gradient lines do not intersect with a region of interest are rejected, while all cells crossed by the gradient lines are incremented with the absolute value of the gradient. In addition to the basic version Bresenham's fast line algorithm is applied to fill cells.
3. After each round, the cell of highest value is found and (following a coarse to fine strategy) the process repeats with a finer accumulator until a sufficiently accurate position is found. To further enhance speed, the supercell of 4 cells with highest energy is selected as new ROI.

3.3 Polar boundary detection

Pupillary and limbic boundary detection is composed of the following steps:

1. The determined center $C = (a, b)$ is used to polar unwrap the iris image I:

$$I_p(r, \theta) := I(a + r \cdot cos(\theta), b + r \cdot sin(\theta)) \quad (1)$$

2. The resulting image is convolved with a set of oriented Gabor kernels ($\lambda = 8\pi, \psi = \frac{\pi}{2}, \sigma = 2, \gamma = 0.1$ and $\theta \in \{-\frac{9\pi}{16}, -\frac{\pi}{2}, -\frac{7\pi}{16}\}$ taking the maximum response for the first iteration, the second iteration used a single kernel with $\theta = -\frac{\pi}{2}, \sigma = 6, \gamma = 1$ only):

$$g(x,y) := \frac{\gamma}{2\pi\sigma^2} \exp\left(-\frac{x'^2 + \gamma^2 y'^2}{2\sigma^2}\right) \cos\left(2\pi\frac{x'}{\lambda} + \psi\right) \tag{2}$$

   where $x' = x\cos(\theta) + y\sin(\theta)$ and $y' = -x\sin(\theta) + y\cos(\theta)$.
3. For a set of equidistant polar angles (i.e. corresponding to the polar image width), the three best vertical filter responses are used for clustering r-values using the k-Means clustering algorithm implemented in OpenCV. The next step determines within each cluster $\mathcal{C}$ the best candidate for each polar angle in the set evaluating an energy function E using the distance to the cluster center c and the convolution result $I_p * g$:

$$E(r,\theta) := 1 - \frac{|r-c|}{\max\limits_{(R,\Theta)\in\mathcal{C}} |R-c|} + \frac{I_p * g(r,\theta)}{\max\limits_{(R,\Theta)\in\mathcal{C}} I_p * g(R,\Theta)} \tag{3}$$

4. The 0.2 and 0.8 quantiles with respect to distance from center are evaluated and all contour points outside the interval are excluded. Finally, missing values are linearly interpolated in polar coordinates from their immediate neighbors.
5. Finally, the contour is fitted with a Fourier series and the result is restricted to the 3 best complex Fourier coefficients, a technique called Fourier based trigonometry proposed by Daugman [6].

Typically, after the first iteration of polar boundary detection, detected boundary curves can be used to derive a better center point C to target clustering errors. Therefore, Pulling and Pushing as proposed by He *et al.* [7] is applied to restore the center point C to its equilibrium within the most pronounced boundary and the polar detection procedure is restarted a second time.

Another problem found with the existing technique was, that typically, the less pronounced boundary was largely affected by noise or eyelids. Therefore, the less expressive boundary is reconstructed from the more stable one, exploiting that both contours exhibit an almost constant distance. In future work, we are planning to refine this technique by performing a fitting of the resulting contour following gradient directions after reconstruction or to perform quality checks, whether the reconstruction really fits better.

Finally, the resulting boundary curves P and L are subjected to Daugman's rubbersheet model, and the resulting iris texture is enhanced using contrast-limited adaptive histogram equalization [14].

4 Experiments

We evaluate segmentation accuracy by assessing the impact on verification recognition accuracy, i.e. ROC curves plotting false acceptance rate (FAR) versus genuine acceptance rate (GAR), given in Fig. 3, using an existing feature extraction

Table 1. Segmentation accuracy and processing time per image.

Algorithm	Equal Error Rate (EER)				Segmentation Time (ST)			
	Casia-I	Casia-L	ND	UBIRIS	Casia-I	Casia-L	ND	UBIRIS
Pcode	**0.74%**	28.77%	22.01%	39.65%	0.49 s	1.96 s	2.29 s	0.18 s
OSIRIS	16.40%	14.89%	**15.45%**	**33.51%**	3.46 s	6.21 s	6.27 s	2.03 s
Proposed	8.07%	**12.90%**	19.04%	34.56%	**0.18 s**	**0.46 s**	**0.48 s**	**0.11 s**

technique. We employ a re-implementation of the feature extraction by Ma *et al.* [11] using dyadic wavelet transform to select local minima and maxima above an adequate threshold in two subbands, yielding a 10240 bit code and Hamming distance for comparison. For rotational alignment issues we applied up to 7-bit circular shifts in each direction. Performance with respect to processing time is evaluated by means of average segmentation time per image for each of the employed databases and listed along with Equal Error Rates (EERs, where $FAR = 1 - GAR$) in Table 1. Furthermore, we evaluate usability by analyzing segmentation errors on different databases in Fig. 4.

For experiments we employ 4 different open iris datasets: (1) *Casia-I* is the left-eye subset of *CASIA-V4*[2] set *Interval* 1332 NIR illuminated indoor images of high quality (320×280 pixel resolution), (2) *Casia-L* consists of a (left-eye) subset of *CASIA-V4* set *Lamp*, 1000 NIR illuminated indoor images of more challenging quality (640×480 pixel resolution), (3) *ND* is a subset from *ND-IRIS-0405*[3], 420 images NIR illuminated indoor images of non-ideal quality (640×480 pixel resolution) , and (4) *UBIRIS* presents the first 100 classes (817 images) in *UBIRIS-V1*[4], highly challenging VW images (200×150 pixel resolution).

We compared the proposed segmentation approach against the following reference implementations: (1) *OSIRIS*[5] is an open source iris segmentation system employing binarization and HT to determine coarsely the pupil region with active contours for refinement. (2) *Pcode*[6] is a custom HT-based segmentation technique, following Masek[7]. It employs (database-specific) contrast adjustment to enhance pupillary and limbic boundaries, Canny edge detection to detect boundary curves and enhancement techniques to remove unlikely edges.

[2] The Center of Biometrics and Security Research, CASIA Iris Image Database, `http://biometrics.idealtest.com`

[3] Computer Vision Research Lab, Univ. of Notre Dame Iris Dataset 0405, `http://www.nd.edu`

[4] Soft Computing and Image Analysis Lab, Univ. of Beira Interior, UBIRIS.v1 dataset, `http://iris.di.ubi.pt/ubiris1.html`

[5] Krichen *et al.*: A biometric reference system for iris. OSIRIS version 2.01, `http://svnext.it-sudparis.eu/svnview2-eph/ref_syst/Iris_Osiris/`

[6] Pschernig: Cancelable biometrics for iris detection with parameterized wavelets and wavelet packets, Masters thesis, Univ. Salzburg, 2009.

[7] Libor Masek, Peter Kovesi. MATLAB Source Code for a Biometric Identification System Based on Iris Patterns. The School of Computer Science and Software Engineering, The University of Western Australia. 2003

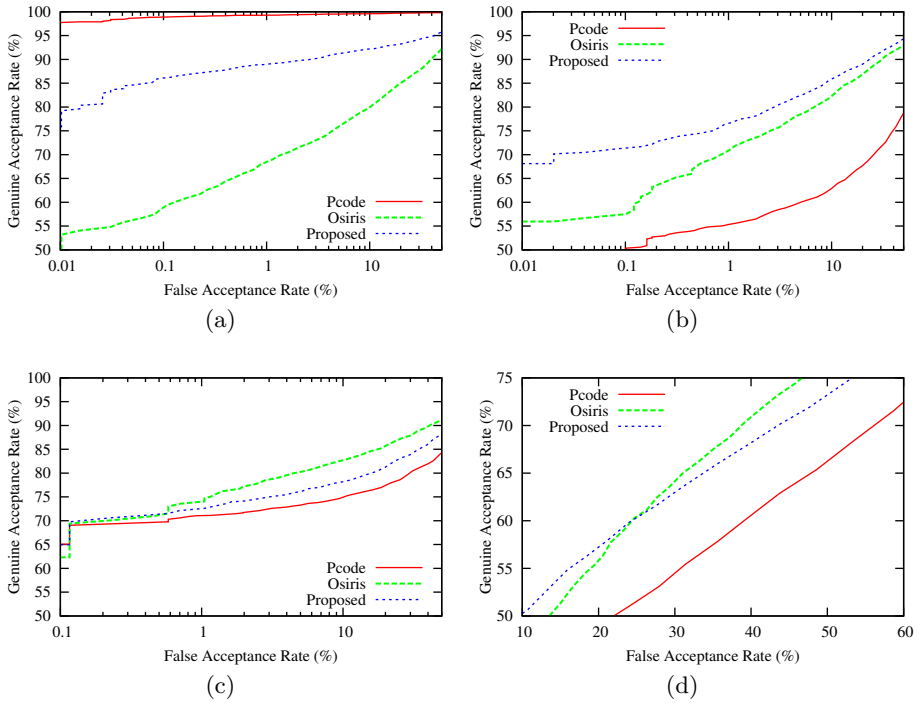

Fig. 3. Impact of segmentation on ROC results using Ma *et al.* 's algorithm on (a) Casia-I (b) Casia-L, (c) ND and, (d) UBIRIS datasets.

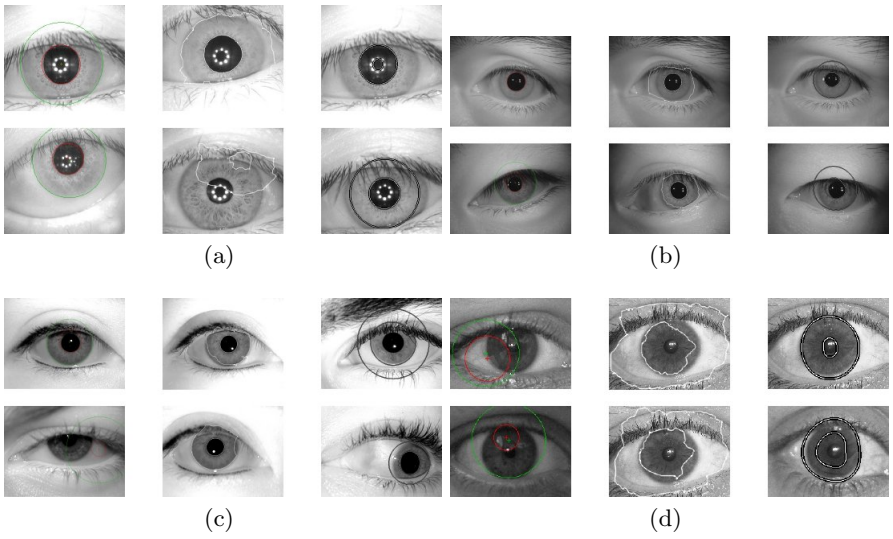

Fig. 4. Segmentation errors of (left) Pcode, (middle) OSIRIS, and (right) proposed method on (a) Casia-I (b) Casia-L, (c) ND and, (d) UBIRIS datasets.

Results on *Casia-I* indicated a best EER of 0.74% at on average 0.49 seconds segmentation time per image (ST) for Pcode. Since this method is explicitly tuned to deliver good results for this database and boundaries can well be represented with circles, this result is expected. The second best accuracy on this set provides the proposed method with 8.07% EER at 0.18 ST. The open OSIRIS approach does not provide very accurate segmentation with 16.4% EER at 3.46 ST also a 20 times higher ST than our method. When inspecting the type of segmentation errors in Fig. 4 made by the algorithms, it is interesting to see, that OSIRIS frequently makes over-segmentation errors (due to less pronounced limbic boundaries) while our proposed method reveals some defects in the classification of pupillary versus limbic boundaries due to circular reflections in the pupillary center and few over-segmentation errors due to sharp collarettes.

For *Casia-L* the proposed method is the most accurate one with 12.9% EER at 0.46 ST, clearly better than OSIRIS (14.89% EER at 6.21 ST) and Pcode (28.77% EER at 1.96 ST). We noticed, that segmentation systems like Pcode tuned to specific image type may fail completely, if assumptions do not hold: its segmentations sometimes fails completely and also many under-segmentation errors occurred due to eyelids. OSIRIS exhibits both over- and under-segmentation errors. For this dataset the reconstruction method assuming concentric centers in the proposed algorithm sometimes causes misplaced reconstructed boundaries. Also misplaced initial centers due to eyelids are critical.

The OSIRIS algorithm being tuned to deliver good results for ICE-2005 also delivers most accurate results (15.45% EER at 6.27 ST) for *ND*, as this represents a superset of ICE-2005. Still, processing takes quite long compared to our method (19.04% EER at 0.48 ST) and even Pcode (22.01% EER at 2.29 ST). The type of segmentation errors made by all three algorithms are comparable to Casia-L, with slightly more stable results provided by OSIRIS.

Finally, in *UBIRIS*, all three techniques provide unsatisfactory results (OSIRIS with 33.51% EER at 2.03 ST, the proposed method with 34.56% EER at 0.11 ST and Pcode with 39.65% EER at 0.18 ST). Interestingly, OSIRIS provides slightly better results, even though it exhibits a systematic error: typically the outer iris boundary is identified as pupillary boundary, so not irides are used for biometric identification, but sclera and surrounding eyelids and eyelashes, which works quite well probably due to the short capturing timespan within each session. While Pcode again exhibits many complete segmentation fails, our algorithm estimates the center quite robust, but again boundary refitting causes some problems.

5 Conclusion

Traditional iris segmentation methods are developed for either VW or NIR images, in order to benefit from strong assumptions with respect to pupil or sclera contrast. However, the growing demand for integrated solutions extracting irides from facial images makes both iris recognition in VW, as well as face recognition in NIR, active research topics demanding for iris segmentation techniques able to

process either type of data. In this work we presented an effective technique with respect to not only accuracy, but also speed and usability, avoiding any overfitting. Experiments confirm, that existing segmentation software in the field is highly affected by the type of iris data.

References

1. Abhyankar, A., Schuckers, S.: Active shape models for effective iris segmentation. In: Proc. of SPIE (2006)
2. Bowyer, K.W., Hollingsworth, K., Flynn, P.J.: Image understanding for iris biometrics: A survey. Computer Vision and Image Understanding 110(2), 281 – 307 (2008)
3. Cauchie, J., Fiolet, V., Villers, D.: Optimization of an hough transform algorithm for the search of a center. Pattern Recognition 41(2), 567–574 (2008)
4. Chen, Y., Adjouadi, M., Han, C., Wang, J., Barreto, A., Rishe, N., Andrian, J.: A highly accurate and computationally efficient approach for unconstrained iris segmentation. Image Vision Computing 28, 261–269 (2010)
5. Daugman, J.: How iris recognition works. IEEE Trans. on Circiuts and Systems for Video Technology 14(1), 21–30 (2004)
6. Daugman, J.: New methods in iris recognition. IEEE Trans. on Systems, Man, and Cybenetics Part B 37(5), 1167–1175 (2007)
7. He, Z., Tan, T., Sun, Z.: Iris localization via pulling and pushing. In: Proc. of the 18th Int'l Conf. on Pattern Recognition. pp. 366–369. ICPR'06 (2006)
8. Labati, R.D., Piuri, V., Scotti, F.: Agent-based image iris segmentation and multipleviews boundary refining. In: Proc. of the 3rd IEEE Int'l Conf. on Biometrics: Theory, Applications and Systems. pp. 204–210. BTAS'09, IEEE Press, Piscataway, NJ, USA (2009)
9. Li, P., Liu, X.: An incremental method for accurate iris segmentation. In: Proc. of the 19th Int'l Conf. on Pattern Recognition. pp. 1–4. ICPR'08 (2008)
10. Luengo-Oroz, M., Faure, E., Angulo, J.: Robust iris segmentation on uncalibrated noisy images using mathematical morphology. Image Vision Computing 28, 278–284 (2010)
11. Ma, L., Tan, T., Wang, Y., Zhang, D.: Efficient iris recognition by characterizing key local variations. IEEE Trans. on Image Processing 13(6), 739–750 (2004)
12. Proenca, H.: Iris recognition: A method to segment visible wavelength iris images acquired on-the-move and at-a-distance. In: 4th Int'l Symp. on Visual Computing (ISVC). pp. 731–742 (2008)
13. Proença, H., Alexandre, L.A.: Iris recognition: Analysis of the error rates regarding the accuracy of the segmentation stage. Image and Vision Computing 28(1), 202–206 (2010)
14. Reza, A.M.: Realization of the contrast limited adaptive histogram equalization (clahe) for real-time image enhancement. J. VLSI Signal Process. Syst. 38(1), 35–44 (2004)
15. Schuckers, S., Schmid, N., Abhyankar, A., Dorairaj, V., Boyce, C., Hornak, L.: On techniques for angle compensation in nonideal iris recognition. IEEE Trans. on Systems, Man, and Cybenetics Part B 37(5), 1176–1190 (2007)
16. Uhl, A., Wild, P.: Weighted adaptive hough and ellipsopolar transforms for real-time iris segmentation. In: Proc. Int'l Conf. on Biometrics (ICB) (to appear, 2012)
17. Wildes, R.P.: Iris recognition: an emerging biometric technology. In: Proc. of the IEEE. vol. 85, pp. 1348–1363 (1997)